JCB Article

Effects of cell tension on the small GTPase Rac

Akira Katsumi,[1] Julie Milanini,[1] William B. Kiosses,[1] Miguel A. del Pozo,[1] Roland Kaunas,[3] Shu Chien,[3] Klaus M. Hahn,[2] and Martin Alexander Schwartz[1]

[1]Division of Vascular Biology and [2]Department of Cell Biology, The Scripps Research Institute, La Jolla, CA 92037
[3]Department of Bioengineering and Whitaker Institute of Biomedical Engineering, University of California San Diego, CA 92093

Cells in the body are subjected to mechanical stresses such as tension, compression, and shear stress. These mechanical stresses play important roles in both physiological and pathological processes; however, mechanisms transducing mechanical stresses into biochemical signals remain elusive. Here, we demonstrated that equibiaxial stretch inhibited lamellipodia formation through deactivation of Rac. Nearly maximal effects on Rac activity were obtained with 10% strain. GAP-resistant, constitutively active V12Rac reversed this inhibition, supporting a critical role for Rac inhibition in the response to stretch. In contrast, activation of endogenous Rac with a constitutively active nucleotide exchange factor did not, suggesting that regulation of GAP activity most likely mediates the inhibition. Uniaxial stretch suppressed lamellipodia along the sides lengthened by stretch and increased it at the adjacent ends. A fluorescence assay for localized Rac showed comparable changes in activity along the sides versus the ends after uniaxial stretch. Blocking polarization of Rac activity by expressing V12Rac prevented subsequent alignment of actin stress fibers. Treatment with Y-27632 or ML-7 that inhibits myosin phosphorylation and contractility increased lamellipodia through Rac activation and decreased cell polarization. We hypothesize that regulation of Rac activity by tension may be important for motility, polarization, and directionality of cell movement.

Introduction

It is well established that mechanical stimuli including gravity, tension, compression, and shear stress are critical to the growth and function of living cells (Ingber, 1997). Mechanical forces may also contribute to pathological states such as atherosclerosis (Davies, 1995), cardiac hypertrophy (Sadoshima and Izumo, 1997), and osteoarthritis (Lane Smith et al., 2000). However, relatively little is known about the molecular mechanisms by which organisms sense mechanical forces and transduce them into biological responses.

Classical studies of cellular responses to forces have demonstrated that neurites grow in response to mechanical tension in tissue culture (Bray, 1984). Fibroblasts were reported to be oriented along the axis of stretch (Haston et al., 1983), and electron microscopic studies indicated that mechanical tension, whether inherent in the cytoskeleton or imposed on the cell surface by exogenous force, can influence the alignment of tight-junction strands (Pitelka and Taggart, 1983). Rearward tension applied by a micropipette in platyfish epidermal cells dramatically suppressed protrusive activity at the leading edge and caused alignment of microfilaments parallel to the applied tension (Kolega, 1986).

Apart from static stretch, cyclic stretch applied to rat cardiac myocytes induces elongation and orientation perpendicular to the direction of the stretch (Terracio et al., 1988). In human umbilical vein endothelial cells, cyclic stretch stimulated stress fiber formation and alignment of cells which involved changes in adenylate cyclase activity (Shirinsky et al., 1989). Cyclic stretch-induced cell orientation was found to depend on calcium influx via stretch-activated cation channels (Naruse et al., 1998), and tyrosine phosphorylation of p130CAS, focal adhesion kinase (FAK)* and paxillin by c-src (Sai et al., 1999), as well as activation of mitogen-activated protein kinase (Wang et al., 2001b) and Rho (Yano et al., 1996).

Cells extend thin, sheet-like processes at their leading edge known as lamellipodia, which contain a dense meshwork of actin filaments. Some lamellipodia extend smoothly outward over the substratum, whereas others move back over the cell surface in a wavelike motion known as ruffling (Bray

Address correspondence to M.A. Schwartz, Department of Vascular Biology, CVN228/VB4, The Scripps Research Institute, 10550 N. Torrey Pines Road, La Jolla, CA 92037. Tel.: (858) 784-7140. Fax: (858) 784-7360. E-mail: schwartz@scripps.edu

Key words: mechanotransduction; mechanical stretch; lamellipodia; polarization; Rac

*Abbreviations used in this paper: ECM, extracellular matrix; FRET, fluorescence resonance energy transfer; GAP, GTPase activating protein; GEF, guanine nucleotide exchange factor; GFP, green fluorescent protein; GST, glutathione *S*-transferase; PBD, the p21-binding domain of PAK1; RBD, the Rho binding domain of Rhotekin; VSM, vascular smooth muscle.

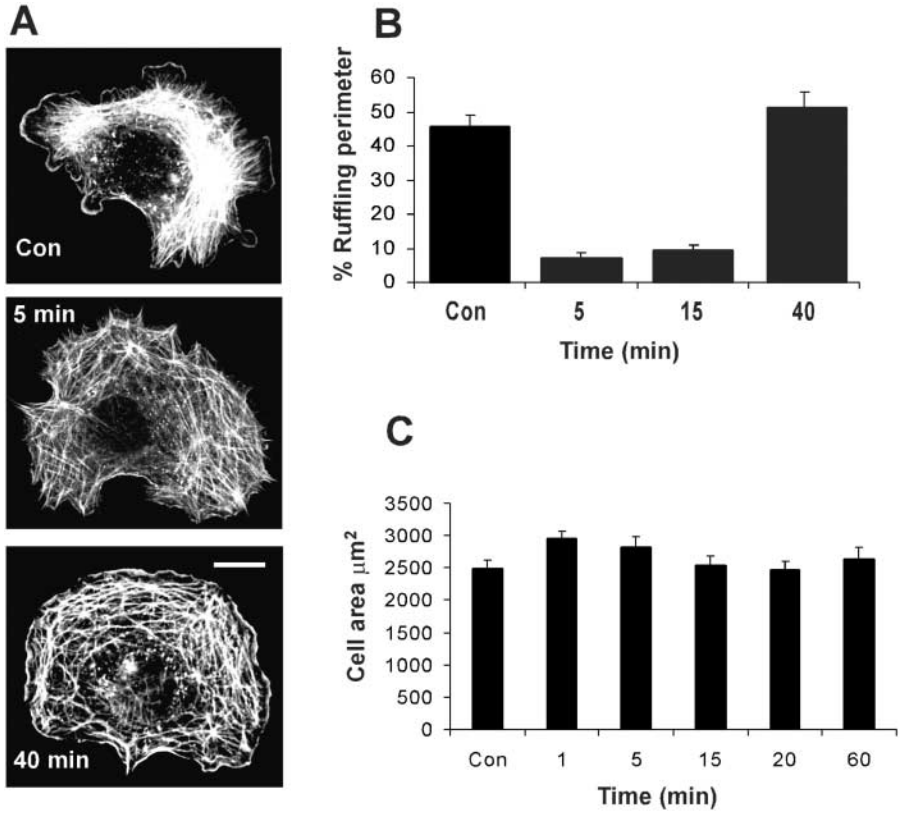

Figure 1. **Equibiaxial stretch inhibits lamellipodia formation.** Rat VSM cells were plated for 3h on collagen-coated silicone membranes in the equibiaxial stretch device. Cells were then stretched to increase area by 15%. (A) At indicated time points cells were fixed and stained with rhodamine-phalloidin. Cells with representative morphologies are shown. Bar, 20 μm. (B) The portion of the cell perimeter occupied by lamellipodia is expressed as percent of the total perimeter. Values are means ± SEM, for 20 cells per data point from three independent experiments. (C) Time-lapse images of VSM cells were recorded and total cell areas before and at various times after stretch were quantified. Values are means ± SEM for 27 cells.

and White, 1988). These structures are regulated by the small GTPase Rac in response to a variety of stimuli, including growth factors and extracellular matrix (ECM) (Schwartz and Shattil, 2000). In the case of ECM, it is striking that cells plated on fibronectin or other adhesive proteins show a marked but transient activation of Rac (Price et al., 1998; del Pozo et al., 2000) that decreases to baseline levels once cells are fully spread. This observation prompted us to consider whether this downregulation of Rac might occur via mechanical effects.

In order to elucidate the effects of mechanical forces on Rac, we applied strain to vascular smooth muscle (VSM) cells and fibroblasts plated on elastic substrata coated with ECM protein. We found that increasing strain via a single step of equibiaxial stretch dramatically decreased lamellipodia due to inhibition of Rac. Conversely, decreasing cell-generated tension by inhibiting myosin phosphorylation increased lamellipodia through Rac activation, suggesting that endogenous tension plays a similar role to regulate Rac. Finally, uniaxial stretch suppressed lamellipodia in a directional fashion. Together with effects of myosin inhibitors, these results indicate that inhibition of Rac depends upon the direction of the tension and suggest that this effect contributes to the polarized morphology of migrating cells.

Results

Effect of equibiaxial strain on lamellipodia formation

We first investigated the effects of mechanical stretch on membrane ruffling and lamellipodia formation, which for the sake of brevity will hereafter be referred to as lamellipodia. Transparent silicone elastic membrane was attached to an equibiaxial stretch device (Lee et al., 1996) and coated with collagen I, which we found to provide better adhesion for VSM cells than fibronectin. Cells were plated for 3 h, at which point they were fully spread but still showed significant lamellipodia. The membranes were then stretched to increase cell area by 15%, which corresponds to a linear strain of ~7% in both directions. Strain was maintained for the duration of the experiment. Subsequent fixation and rhodamine-phalloidin staining revealed that the increased strain caused a marked inhibition of lamellipodia that recovered at later times (Fig. 1 A). To quantify the effects, the fraction of the cell perimeter occupied by lamellipodia was measured. This analysis showed that increasing strain triggered a transient inhibition of lamellipodia followed by recovery at later times (Fig. 1 B). Experiments with NIH3T3 cells and primary mouse embryo fibroblasts showed similar results (unpublished data). The average cell area (μm^2) was measured from time-lapse images (Fig. 1 C). We observed that cell area increased by the expected amount shortly after applying strain. Cell area then started to decrease due to retraction and returned to their original size by ~20 min. Time-lapse image of stretched VSM cells demonstrated that cells showed loss of lamellipodia within 1 min after being stretched. Lamellipodial extension was reinitiated only after cells completed the retraction and returned to their original size (unpublished data). Thus, the transient inhibition of lamellipodia corresponds to the period during which cells experience increased strain.

Effect of equibiaxial strain on Rac activity

To investigate whether Rac is involved in this finding, pull-down assays for GTP-bound Rac were performed (del Pozo

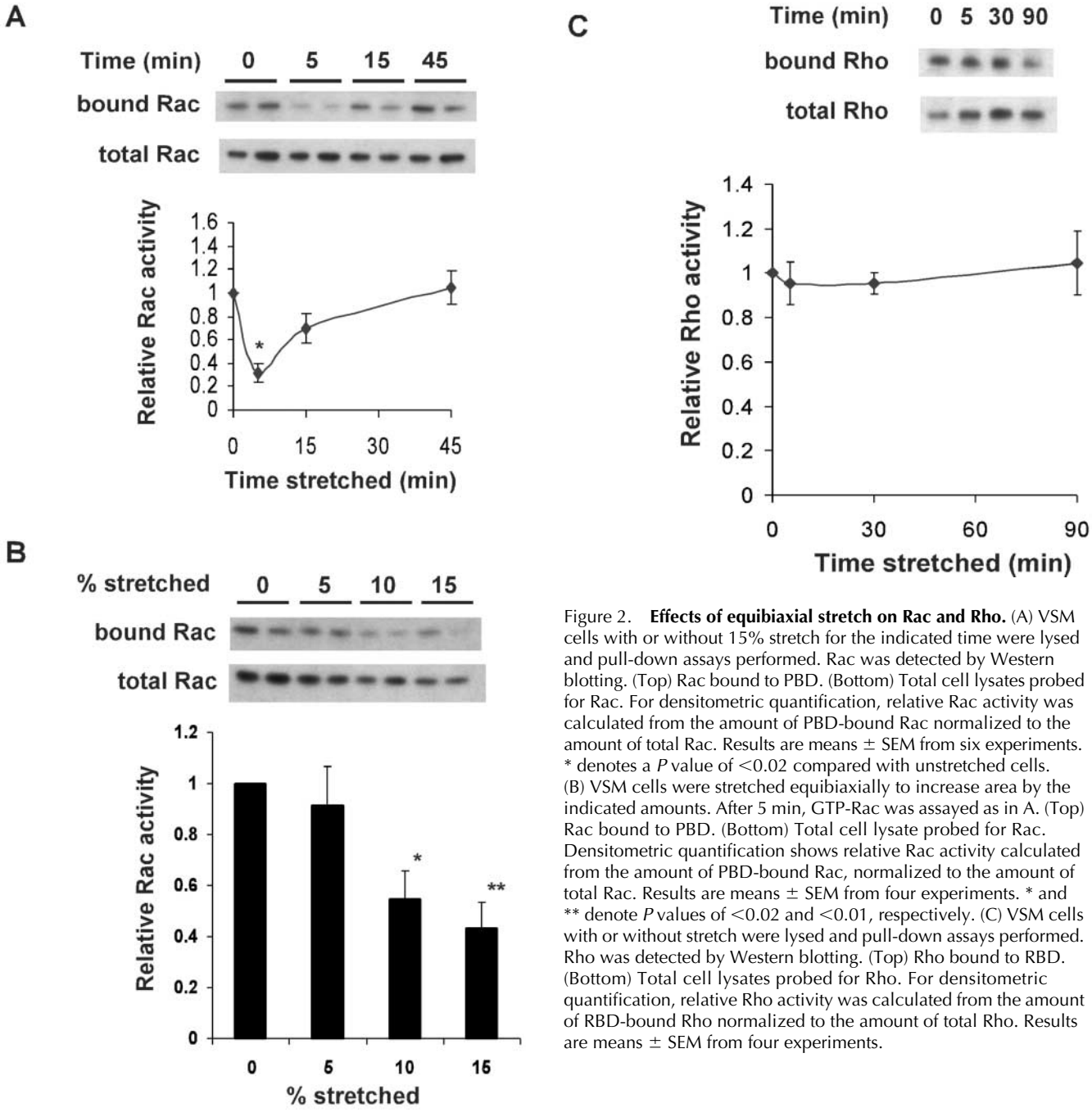

Figure 2. **Effects of equibiaxial stretch on Rac and Rho.** (A) VSM cells with or without 15% stretch for the indicated time were lysed and pull-down assays performed. Rac was detected by Western blotting. (Top) Rac bound to PBD. (Bottom) Total cell lysates probed for Rac. For densitometric quantification, relative Rac activity was calculated from the amount of PBD-bound Rac normalized to the amount of total Rac. Results are means ± SEM from six experiments. * denotes a P value of <0.02 compared with unstretched cells. (B) VSM cells were stretched equibiaxially to increase area by the indicated amounts. After 5 min, GTP-Rac was assayed as in A. (Top) Rac bound to PBD. (Bottom) Total cell lysate probed for Rac. Densitometric quantification shows relative Rac activity calculated from the amount of PBD-bound Rac, normalized to the amount of total Rac. Results are means ± SEM from four experiments. * and ** denote P values of <0.02 and <0.01, respectively. (C) VSM cells with or without stretch were lysed and pull-down assays performed. Rho was detected by Western blotting. (Top) Rho bound to RBD. (Bottom) Total cell lysates probed for Rho. For densitometric quantification, relative Rho activity was calculated from the amount of RBD-bound Rho normalized to the amount of total Rho. Results are means ± SEM from four experiments.

et al., 2000). VSM cells were incubated in 10% FBS/DME, spread on collagen-coated membranes in the equibiaxial stretch device for 3 h, and subjected to 15% strain. Lysates were prepared and the amount of Rac precipitated with the p21-binding domain of PAK1 (PBD) fused to glutathione *S*-transferase (GST) (GST–PBD) was determined by Western blotting. The results showed that equibiaxial stretch caused a transient decrease in the levels of activated Rac (Fig. 2 A). Inhibition was maximal at 5 min and Rac activity recovered to the prestretched level by 45 min. Mouse embryo fibroblasts gave similar decreases in Rac activity (unpublished data). These data are consistent with the changes in lamellipodia. Serum-starved VSM cells showed lower baseline levels of Rac activity, but the response to strain was qualitatively similar (unpublished data). Next we investigated the dose–response relationship between mechanical strain and Rac activity. The experiments showed that 10% strain had nearly maximal effects on Rac activity (Fig. 2 B). In contrast, there was no significant change in Rho activity (Fig. 2 C).

Differential effects of V12Rac versus Tiam1

To further investigate the role of Rac in the strain-induced decrease of lamellipodia, we tested whether activating Rac could reverse the inhibition. A DNA expression construct for green fluorescent protein (GFP)-V12Rac was transfected into VSM cells and strain applied as before. V12Rac-expressing cells showed extensive lamellipodia before stretch

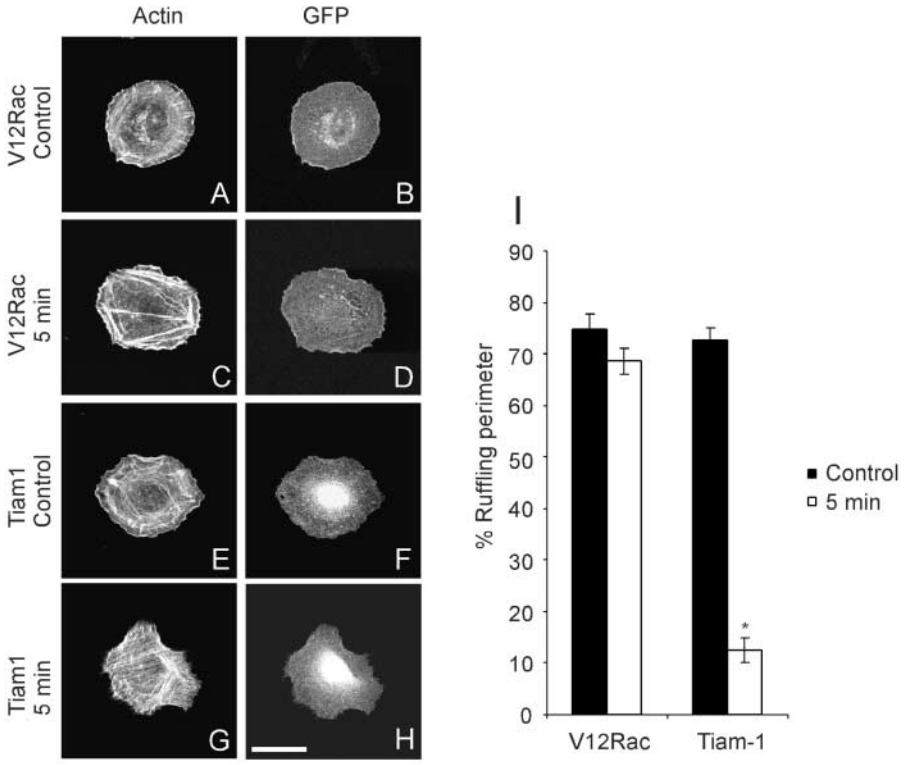

Figure 3. **Effects of stretch on V12Rac- and Tiam1-transfected VSM cells.** (A–D) VSM cells were transfected with 2 μg of pEGFP-C1-V12Rac. (E–H) VSM cells were cotransfected with 1.6 μg of pcDNAINeo-Tiam1 and 0.4 μg of pEGFP. At 24 h after transfection, cells were plated on collagen I–coated silicone membrane for 3 h and stretched equibiaxially by 15% for 5min. Fluorescence images of actin filaments (A, C, E, and G) and GFP (B, D, F, and H) in the same cells were shown. Results are representative of three experiments. Bar, 20 μm. (I) The portion of the cell perimeter occupied by lamellipodia is expressed as percent of the total perimeter. Values are means ± SEM, for 20 cells per data point. * indicates $P < 0.01$.

(Fig. 3, A and B), which was unaffected by 15% equibiaxial stretch (Fig. 3, C and D). Some changes in appearance of lamellipodia were noted, as well as increased intensity of the actin stress fibers, but no decrease in lamellipodia was detected. This result supports the conclusion that the decrease in Rac activity mediates the inhibition of lamellipodia.

The V12 mutant of Rac is deficient in both endogenous and stimulated GAP activity, leading to its constitutive activation. However, there are two main mechanisms to deactivate Rac: either activation of GTPase activating proteins (GAPs), or deactivation of guanine nucleotide exchange factors (GEFs). To distinguish these two possibilities, we activated endogenous Rac by expression of a constitutively active GEF. Cells were transfected with a vector coding for NH_2-terminally truncated Tiam-1, a GEF specific for Rac (van Leeuwen et al., 1995), together with GFP as a marker. Expression of Tiam-1 in VSM also induced extensive lamellipodia (Fig.3, E and F). However, when subjected to stretch, Tiam-1 transfectants showed a marked decrease in lamellipodia after strain (Fig. 3, G and H), in sharp contrast to V12Rac transfectants. Quantification showed that equibiaxial stretch significantly decreased lamellipodia in Tiam-1–expressing cells, whereas V12Rac-expressing cells were not affected (Fig. 3 I). Although we cannot exclude the possibility that truncated and activated Tiam-1 is also affected by stretch, these results suggest that activation of GAP(s) rather than deactivation of GEF(s) is most likely responsible for the downregulation of Rac by equibiaxial strain.

Effects of uniaxial stretch

Biaxial strain includes both a radial component (i.e., perpendicular to cell edges), and a tangential component (i.e., parallel to cell edges). Thus, biaxial strain does not address whether the direction of the applied strain is important. Therefore, we investigated the effects of uniaxial stretch on lamellipodia. VSM cells were spread on collagen-coated membranes in a device that applies stretch in one dimension as described in Materials and methods. Cells at 75 min after plating were well spread but remained largely circular and unpolarized, thus changes in polarity induced by strain could be easily assessed. Cells were then stretched to increase length by 8%. Strain was maintained for the duration of the experiment as before. Time-lapse images (Fig. 4 A) showed that cells immediately after stretch had increased their length in the direction of strain as expected. Quantitative analysis of the effects on cell size also revealed some decrease in size perpendicular to stretch (Fig. 4 C, 0 min). This change in area reflects the combination of tensile strain in the direction of stretch and a smaller amount of compression in the perpendicular direction, usually ~15% of the increase (Sadoshima et al., 1992; Lee et al., 1999).

Immediate changes in cell shape directly due to the change in strain are shown in Fig. 4 C (0–1-min interval). Surprisingly, after this initial strain, the cells continued to extend in the direction of strain (i.e., along the ends), while showing some further retraction perpendicular to the direction of applied strain (i.e., along the sides) (Fig. 4, 1–5-min interval). This result is displayed in Fig. 4 B, where regions that increased between 1 and 5 min are colored red, and regions of retraction are shown in blue. Quantitative analysis for multiple cells in Fig. 4 C clearly indicates that uniaxial stretch increased the membrane protrusive activity at the ends and induced some retraction along the sides in the 1–5-min interval. This result is consistent with a decrease in Rac activity at regions that experienced tangential strain (sides) and an increase of Rac activity at the edges that experienced

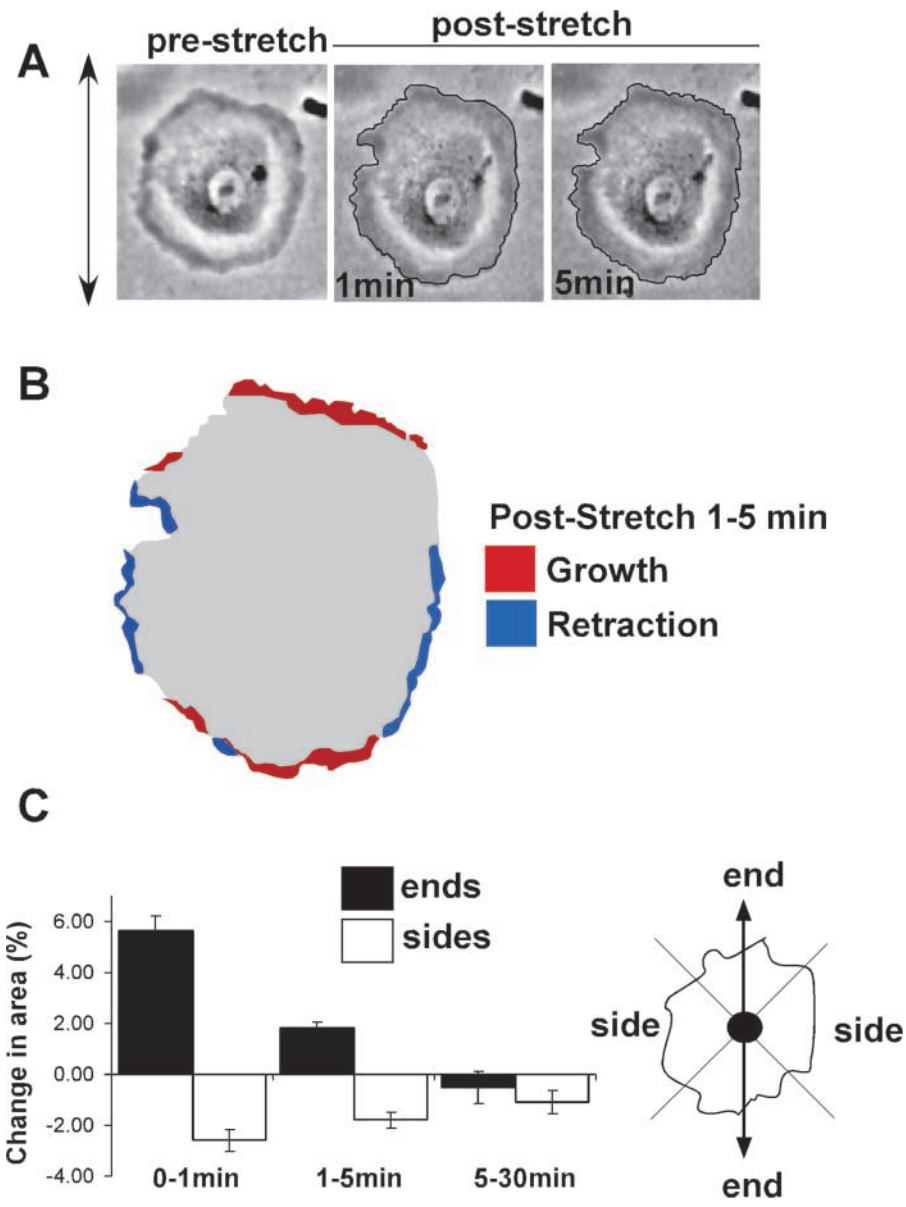

Figure 4. **Effects of uniaxial stretch on membrane protrusive activity.** (A) VSM cells were plated on collagen I–coated silicone membrane for 75 min. Cells were then stretched uniaxially by 8%, and phase-contrast images recorded. (B) Schematic representation of the cell in (A). The area that increased between 1 and 5 min after stretch is shown in red, and the area retracted during the same period is shown in blue. (C) Average increases or decreases in area during the specified interval after stretch were calculated for ends and the sides. Values are mean ± SEM for 80 cells from four independent experiments.

radial strain (ends). VSM cells under 17% uniaxial stretch showed similar results (unpublished data). Unstretched control cells did not change area significantly over the same period (unpublished data).

We also stained cells for actin at later times after uniaxial strain to score the direction of stress fibers. The angles ± 45° in the direction of stretch define "parallel, " whereas the opposite quadrant (45–135°) defines "perpendicular." Stress fibers with no predominant direction were scored as "random". Alignment of stress fibers in the direction of stretch increased significantly at 30 and 60 min (Fig. 5, A and B). Additionally, the focal adhesion proteins α-actinin and vinculin were observed to redistribute, decreasing along the sides and increasing at the ends (unpublished data). To investigate the relationship between early effects on Rac and later effects on alignment of stress fibers, cells expressing V12Rac, which prevents Rac inhibition by stretch, were subjected to uniaxial strain. V12Rac completely blocked alignment of stress fibers after stretch (Fig. 5, C and D). This result strongly suggests that polarized Rac activity is required for the subsequent alignment of stress fibers.

In situ Rac assay

The above results suggest that Rac in different regions of a cell may be differentially affected by an asymmetric strain. To investigate this idea we turned to a recently developed fluorescence resonance energy transfer (FRET) assay for local Rac activity (Kraynov et al., 2000). The assay is based on the principle that upon activation, GFP-labeled Rac binds to Alexa-PBD, resulting in an increase in FRET that can be imaged in the microscope.

In these experiments, VSM cells containing GFP-Rac and Alexa-PBD were plated on collagen- coated membranes for 75 min as above. When FRET was determined, we observed that most of the cells had zones of high Rac activity near cell edges, though the cells were generally circular and nonpolarized (Fig. 6 A, top). Cells also showed a substantial level of perinuclear Rac activity. This pool was also observed by

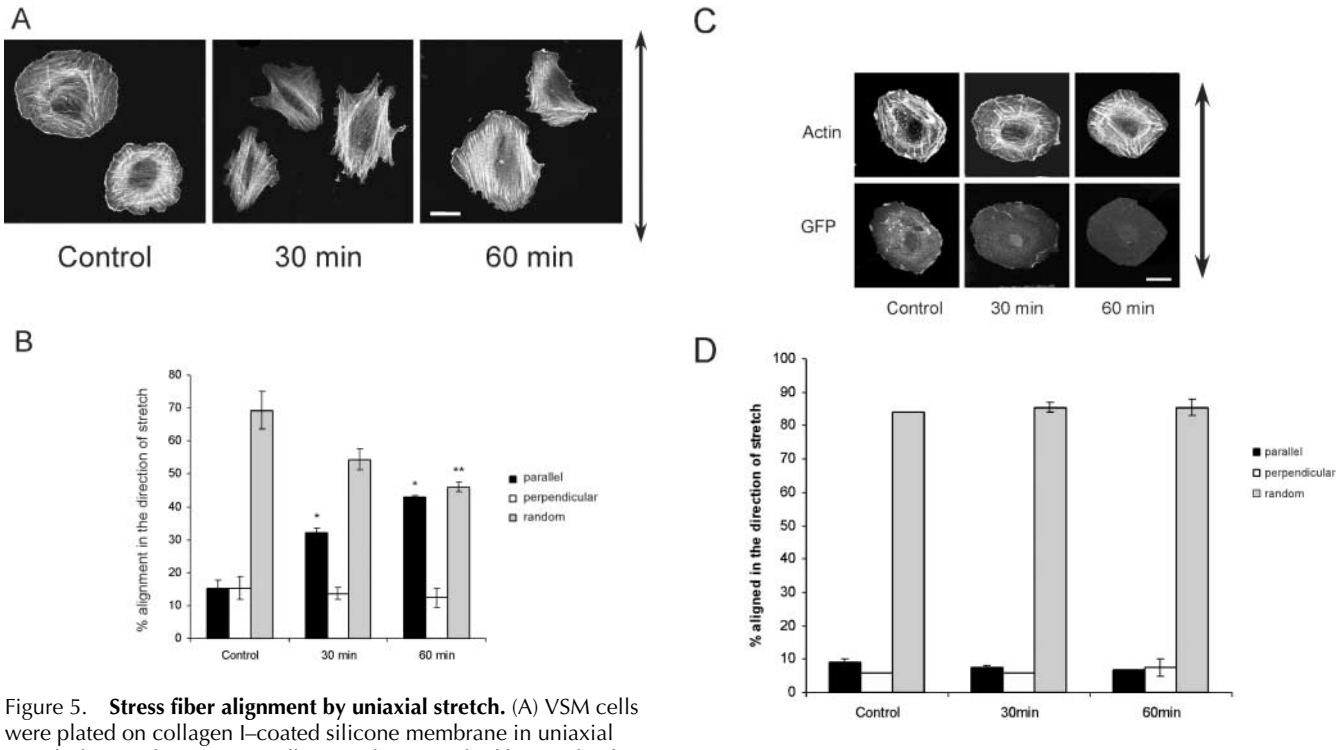

Figure 5. **Stress fiber alignment by uniaxial stretch.** (A) VSM cells were plated on collagen I–coated silicone membrane in uniaxial stretch devices for 75 min. Cells were then stretched by 8% for the time indicated, fixed, and stained with rhodamine-phalloidin. The arrow indicates the direction of stretch. Bar, 20 μm. (B) Cells were scored for whether the main direction of stress fibers was parallel or perpendicular (± 45°) to the direction of stretch. For each time point, 100 cells were scored. Results are means ± SEM from three independent experiments. * and ** denote $P < 0.05$ or 0.02, respectively, compared with control. (C) VSM cells were transfected with pEGFP-C1-V12Rac. Cells were plated on collagen I–coated silicone membrane in uniaxial stretch devices for 75 min. Cells were then stretched by 8% for the time indicated. Fluorescence images of actin filaments and GFP in the same cells were shown. The arrow indicates the direction of stretch. Bar, 20 μm. (D) The alignment of stress fibers was assessed as before for 100 cells per time point. Results are means ± range from two independent experiments.

Kraynov et al. (2000) and did not noticeably change in response to extracellular signals. The nature of this compartment is presently unknown but does not correlate with lamellipodia. Examination of FRET near cell edges showed that uniaxial strain (8% increase in length) induced an increase in GTP-bound Rac at the ends and a decrease at the sides (Fig. 6 A, bottom). The total levels of FRET near cell edges did not change substantially until much later times when Rac activity diminished as it usually does at later times after cell spreading (Price et al., 1998; del Pozo et al., 2000).

To quantify these effects, images were analyzed by dividing cells into four quadrants as diagramed in Fig. 4 C. Cells were first scored for whether the FRET signal was unpolarized (i.e., circular), primarily at the ends or primarily along the sides. Fig. 6 B shows that uniaxial strain induced a dramatic increase in the fraction of cells that were polarized in the direction of applied strain. The polarization was maximal at short times and then dissipated. To assess this polarization in a completely unbiased way, the number of pixels and pixel intensity within the areas of FRET near cell edges was quantified. The total signal above the background was calculated for both the sides and ends as defined by the quadrants as before. These results (Fig. 6 C) demonstrate a decrease of Rac activity along the sides with an increase at the ends. Taken together, these results demonstrate that stretch inhibits Rac in a vectorial manner, inhibiting Rac along the sides that are lengthened by the applied strain. There is also an increase in FRET on the ends, which may be due to the smaller compression in this direction. These results therefore agree with assays of membrane protrusiveness (Fig. 4). They indicate that tangential strain is the critical regulator of Rac whereas radial strain is less effective.

Effects of Y-27632 and ML-7 on lamellipodia

It is likely that the applied strain acts by increasing tension in specific elements within cells. Consequently, we investigated whether cell-generated tension functioned similarly to the externally applied strain in suppressing Rac activity. Therefore, inhibitors of myosin phosphorylation were examined. Blockade of Rho-kinase with Y-27632 or myosin light chain kinase with ML-7 is known to decrease cell-generated tension via distinct mechanisms (Zhong et al., 1997; Narumiya et al., 2000). Treatment of VSM cells for 60 min with either of these compounds moderately, but significantly increased Rac activity (Fig. 7, A and B). Staining of actin filaments in treated cells showed increased lamellipodia in cells treated with Y-27632 or low doses of ML-7 (Fig. 7 C). Y-27632 caused a noticeable but incomplete disassembly of stress fibers (Fig. 7 C). Higher doses of ML-7 (10 μM) caused disassembly of actin stress fibers and collapse of lamellipodia (unpublished data). Presumably, myosin phosphorylation is required for lamellipodia, which are therefore inhibited at higher doses of ML-7.

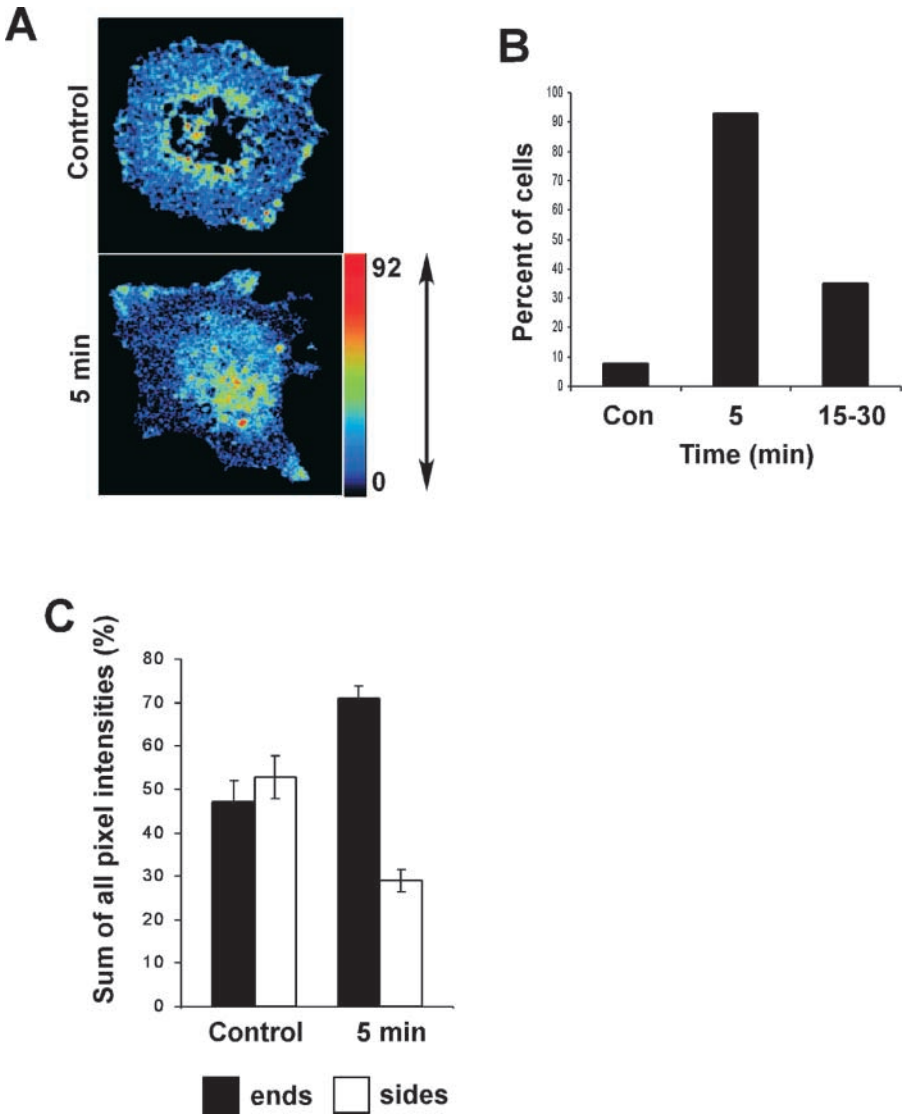

Figure 6. **FRET assay for GTP-Rac.** VSM cells containing wild-type Rac-GFP and Alexa-PBD protein were analyzed. (A) Corrected FRET images are representative of five independent experiments. A color scale corresponding to FRET intensity on a scale of 0–92 is displayed. Red represents high and blue low FRET signal. (B) Scoring polarization. Cells with positive FRET signals near edges were divided into quadrants as for Fig 4. They were scored to assess whether FRET was predominantly localized to ends, as opposed to remaining unpolarized or localizing to the sides. Values represent the percent of cells where FRET is predominantly at the ends. Approximately 50 cells were scored for each time point. (C) Positive zones at cell edges were outlined and the sum of all pixel intensities within these areas was calculated. The fraction of the total FRET signal within the ends and side quadrants were calculated for each cell and expressed as percent of the total. Values are means ± SEM, for ~50 cells at each point.

Migratory cells in culture often show a polarized morphology in which the leading edge forms lamellipodia, whereas the sides and rear are quiescent. To further characterize these effects, VSM cells on coverslips that showed a polarized morphology were examined by time-lapse imaging. Addition of 10 μM Y-27632 increased lamellipodia and caused a loss of the polarized morphology (Fig. 8 A). Quantitative analysis showed that most of the increased lamellipodia appeared in the tail region, which is normally quiescent (Fig. 8, B and C). ML-7 at 1 μM had very similar effects (Fig. 9). Both Y-27632 and ML-7 decreased cell-generated tractional forces (by >50%) and slightly increased cell area (by ~4%), but the change in area did not reach statistical significance. Addition of 10% FBS to serum-starved VSM cells increased total lamellipodia; however, it neither increased lamellipodia in the tail region nor diminished the polarized morphology (unpublished data). The observation that decreasing endogenous myosin-dependent tension increases Rac activity indicates that endogenous tension must inhibit Rac to a significant degree. The results also suggest that tension contributes to polarity of Rac activity and cell morphology.

Discussion

To study the effects of stretch on membrane protrusions, we subjected cells plated on elastic substrata to mechanical strain. Our results show first that equibiaxial stretch inhibited formation of lamellipodia and decreased Rac activity. Increasing cell area by 10% showed nearly maximal effects on Rac activity, suggesting that this phenomenon may occur under physiological conditions (Wilson et al., 1995; Lee et al., 1996). Rescue of this phenotype by V12Rac supports the concept that Rac inhibition is responsible for cessation of lamellipodia formation. The result that constitutively active Tiam-1 failed to rescue this phenotype suggests that changes in activity of a GAP may mediate the effect of mechanical stretch on Rac activity.

When cells are subjected to externally applied strain, there are two factors that could conceivably regulate signal transduction. The displacement of the cell edges could itself directly affect Rac, or alternatively, the resultant increase in tension within the cytoskeleton or membrane could be the critical factor. We found that treating cells with Y-27632 and ML-7 did not cause any significant displacement of cell edges that could account for the increase, whereas they did

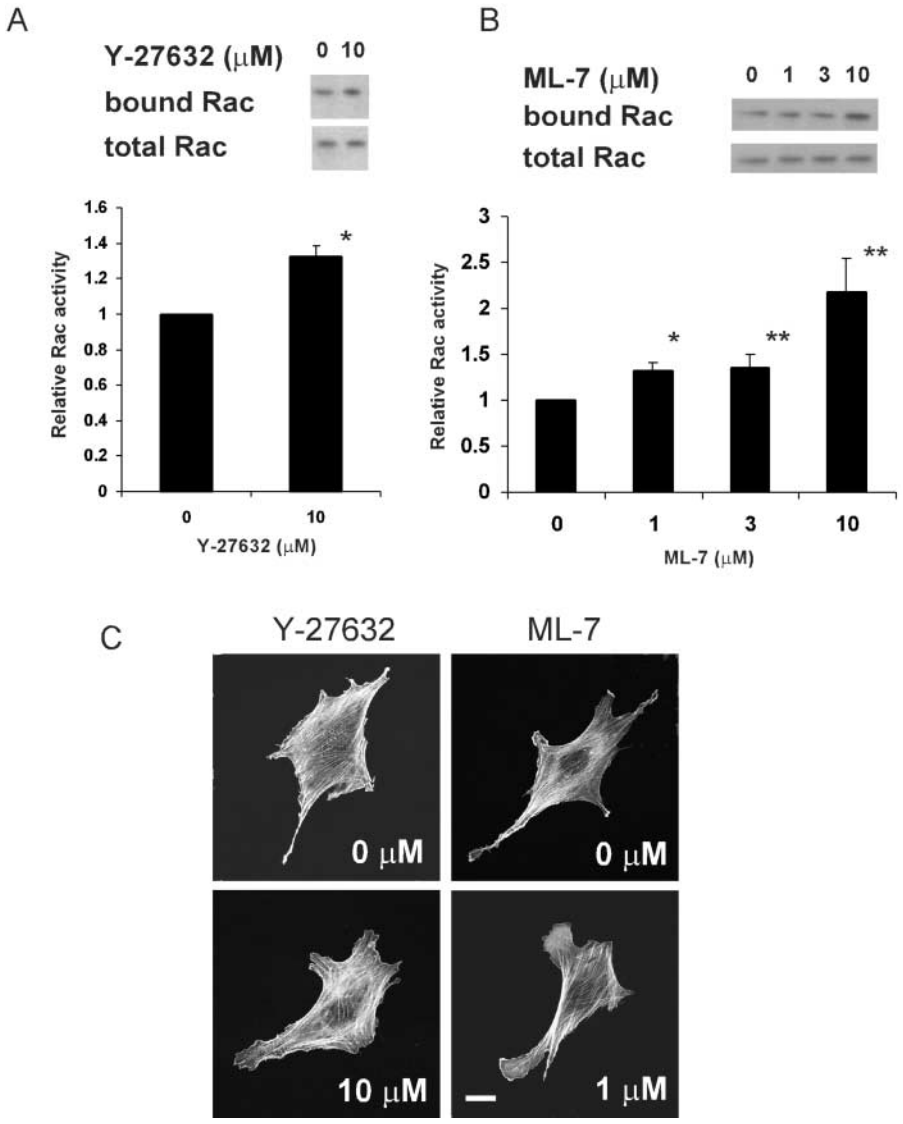

Figure 7. **Effects of Y-27632 and ML-7 on Rac activity.** VSM cells were spread on collagen I–coated coverslip for 16 h, and were incubated with indicated concentrations of Y-27632 (A) or ML-7 (B) for 1 h. Cells were then lysed and GTP-bound Rac and total Rac was detected using the pull-down assay. For densitometric quantification, values are means ± SEM from three experiments. * and ** denote $P < 0.02$ or <0.05 relative to control, respectively. (C) VSM cells treated with indicated amounts of Y-27632 or ML-7 for 1 h were fixed and stained with rhodamine-phalloidin. Bar, 20 μm.

decrease cell tension applied to the substratum. Thus, altering tension under conditions where displacement is relatively constant also affects Rac activity, suggesting that tension within a cell transduces the signal to Rac.

The effect of tension on Rac may explain published observations from many systems. NIH3T3 cells plated on flexible substrates exert less tension and also show increased rates of lamellipodial activity and motility compared with cells on rigid substrates (Pelham and Wang, 1997). Adhesion of fibroblasts to surfaces coated with high concentrations of fibronectin inhibited Rac activation and decreased migration compared with moderate coating densities (Cox et al., 2001). In that study, Rac inhibition was linked to high Rho activity, which is a major determinant of myosin phosphorylation and contractility, again consistent with our findings. The well-known alignment of cells in response to stretch is also consistent with the effects reported here, as are developmental processes in which tractional fields govern cell migration and organization of cells into higher order structures (Davis and Camarillo, 1995; Ingber and Folkman, 1989).

Our results also demonstrated that with uniaxial strain, protrusive activity increased at the ends and decreased along the sides. The results of the in situ Rac assay also demonstrated that Rac is decreased at the edges that are subjected to increased tangential tension (i.e., the edges that actually lengthened). This is consistent with the previous finding that tension applied to the cell suppresses lateral protrusive activity (Kolega, 1986). The opposite edges that do not lengthen should experience increased radial tension, consequently this component must be less effective at inactivating Rac. Uniaxial stretch by 17% did not dramatically inhibit total protrusive activity, in sharp contrast with 15% equibiaxial stretch. These results demonstrated that direction of applied tension rather than increase in area is critical for the effects on Rac.

These observations also precisely match the morphology of cells under normal conditions and the effects of myosin inhibitors. Previous studies have shown that cell-generated tension is strongest along the front–rear axis of migrating cells (Galbraith and Sheetz, 1997; Pelham and Wang, 1999; Balaban et al., 2001). Cells under normal conditions extend lamellipodia primarily at edges perpendicular to actin stress fibers, whereas edges parallel to stress fibers that should experience tangential tension are inhibited. Therefore, one

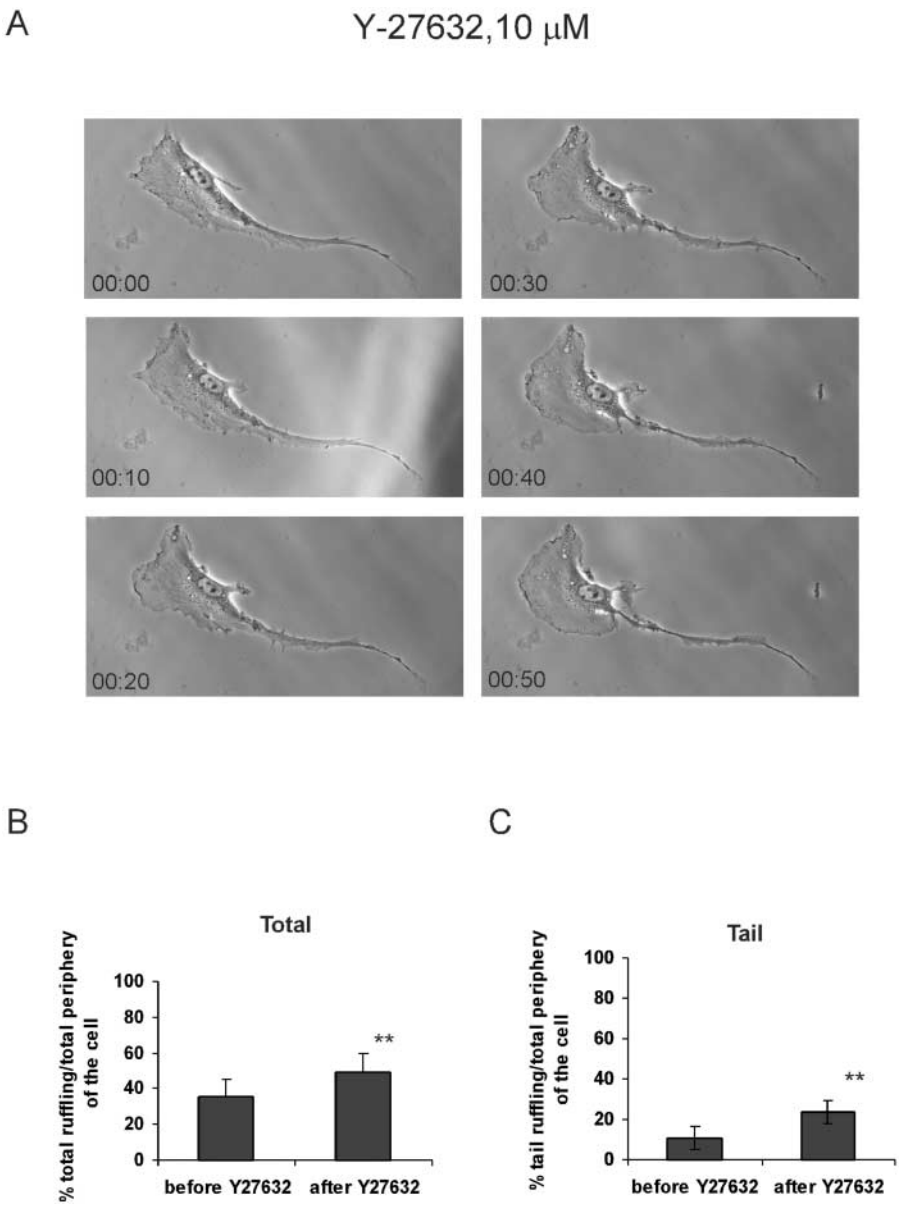

Figure 8. **Y-27632 stimulates lamellipodia and disrupts polarity.** VSM cells were plated on coverslips coated with collagen I. (A) Time-lapse images of cells at the indicated time points before and after the addition of 10 μM Y-27632 are shown. The total (B) and tail (C) lamellipodia was quantified as described in the Materials and methods. Values are means ± SEM for 10 cells per each condition from four independent experiments. ** denotes $P < 0.02$.

would predict that endogenous tension should inhibit Rac along the sides parallel to the direction of migration, which should help maintain the typical morphology of migrating cells. We observed that decreasing endogenous myosin-dependent force generation not only increased Rac activity, but specifically increased lamellipodia along the sides and tail to decrease polarity. These results demonstrate that cell-generated tension regulates Rac and suggest that this regulation contributes to cell polarity.

At later times, we observed redistribution of focal adhesion proteins. This observation is consistent with previous findings demonstrating that mechanical stretch induces focal adhesion assembly (Riveline et al., 2001; Wang et al., 2001a). The alignment of actin stress fibers in the direction of the applied stretch was seen at later time (30–60 min). V12Rac completely blocks alignment of stress fiber after uniaxial stretch. This strongly suggests that early effects on Rac by uniaxial stretch is upstream of stress fiber alignments at later time. Further studies aiming to determine the signaling events that mediate regulation of Rac by tension are of particular interest in elucidating fundamental mechanisms of mechanotransduction.

Materials and methods

Materials

Reagents were purchased from Sigma-Aldrich unless otherwise noted. Y-27632 and ML-7 were purchased from Calbiochem. Transparent silicone elastic membrane was purchased from Specialty Manufacturing, Inc.

Cell culture and DNA transfection

Rat aortic smooth muscle (VSM) cells, NIH3T3 cells and mouse embryonic fibroblasts were maintained in DME (Life Technologies) containing 10% FBS unless otherwise indicated. Cells were cultured at 37°C in a humidified incubator containing 7% carbon dioxide. Transient transfections were performed using Effectene reagents (QIAGEN) according to the manufacturer's instructions. pcDNAINeo-Tiam1 was provided by John G. Collard (The Netherlands Cancer Institute, Amsterdam, The Netherlands). GFP-V12Rac was described previously (del Pozo et al., 1999).

Stretch devices

The equibiaxial stretch device was previously described (Lee et al., 1996). Briefly, a silicone elastic membrane is attached to the membrane

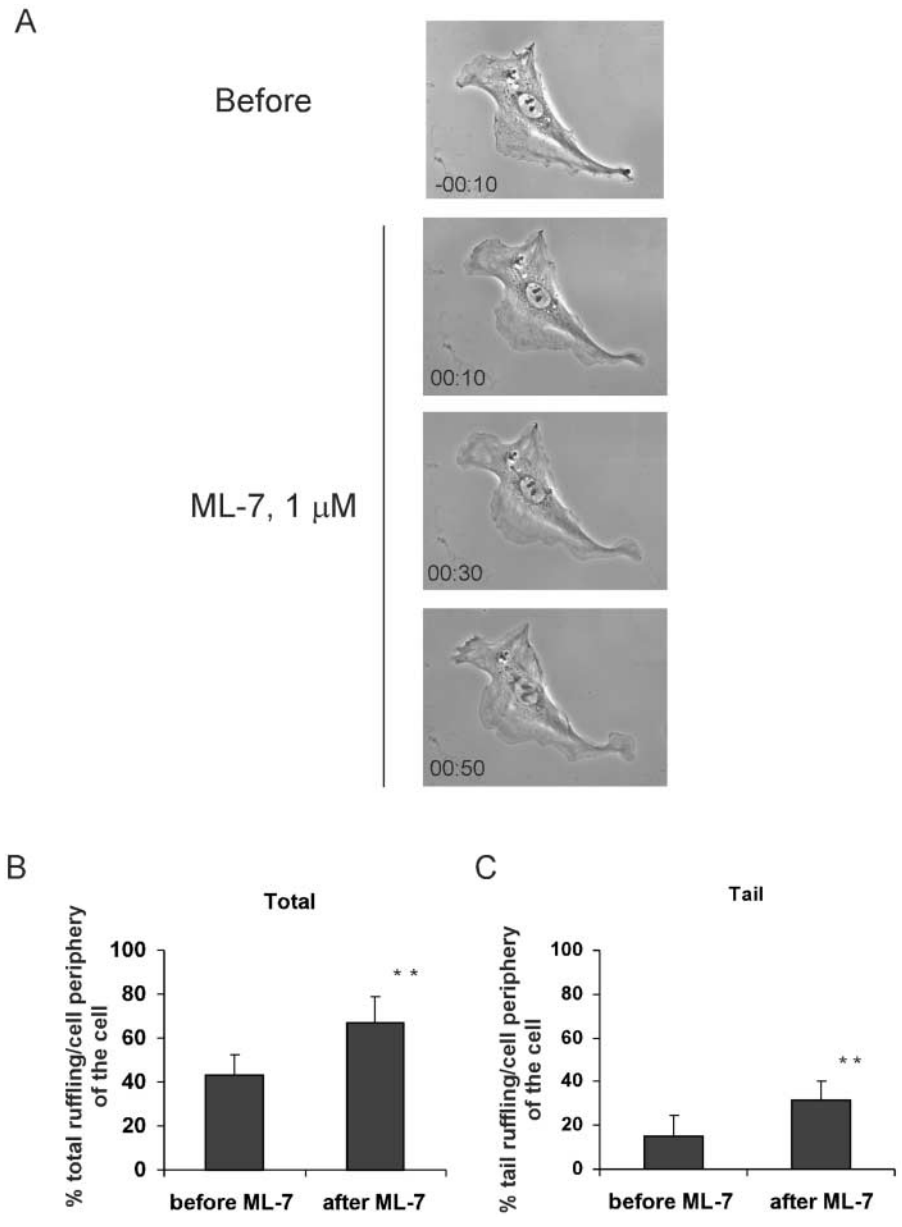

Fig. 9. **ML-7 stimulates lamellipodia and disrupts polarity.** VSM cells were plated on coverslips coated with collagen I. Time-lapse images of cells at the indicated time point after the addition of 1 μM ML-7 are shown (A). The total (B) and tail (C) lamellipodia was quantified as described in the Materials and methods. Values are means ± SEM for 10 cells per each condition from four independent experiments. ** denotes a $P < 0.02$.

holder to form the bottom of the device. Indentation of the ring against the membrane results in a homogenous plane equibiaxial stretch of the membrane. Strains along circumferential and radial axes were equal in magnitude and homogenously distributed, and two-dimensional strains in the stretched cells were not significantly different from mean equibiaxial strains measured in the substrate for nominal strains up to 10% (Lee et al., 1996). The uniaxial stretch devices were similar to previously described instruments (Lee et al., 1999). In brief, a rectangular membrane is attached to rigid supports at either end, while the sides are free. Strain is applied by increasing the distance between the ends with a pair of stainless steel rods and screws. The displacement of markers during stretch was measured in microscopic digital images using a 4× objective, showing the strain in the direction parallel to the stretch axis has no significant difference at various points measured. Compression perpendicular to the axis of stretch did vary; for an 8% stretch it was 2.2% in the center of the membrane and decreased to 0.1% at the edges. Cells were examined close to the center for all experiments. For both types of devices, the strain was applied over ~10 s, which is the time required to manually turn the ring or screws. Strain remained constant for the duration of the experiments. For VSM cells, membranes in the devices were coated with a solution of 40 μg/ml collagen type I for 2 h, and then sterilized by irradiation under the UV light in a laminar flow hood for 15 min. For fibroblasts membranes were coated with 20 μg/ml fibronectin using the same protocol.

GTPase assays

Rac assays were performed as described (del Pozo et al., 2000). Treated cells were washed with ice-cold PBS and lysed in 400 μl buffer containing 0.5% NP-40, 50 mM Tris, pH 7.0, 500 mM NaCl, 1 mM $MgCl_2$, 1 mM EGTA, 1 mM PMSF, 1 μg/ml aprotinin, 1 μg/ml leupeptin, and 20 μg GST–PBD. Lysates were centrifuged to remove particulates and incubated with glutathione-agarose beads (Sigma-Aldrich) for 30 min at 4°C, washed three times, and eluted with SDS sample buffer. Rac protein was detected by Western blotting using a monoclonal antibody against Rac1 (Upstate Biotechnology). Rho assays were performed as described (Ren et al., 1999). Treated cells were washed with ice-cold phosphate-buffered saline and lysed in 400 μl RIPA buffer (50 mM Tris, pH 7.2, 1% Triton X-100, 0.5% sodium deoxycolate, 0.1% SDS, 500 mM NaCl, 10 mM $MgCl_2$, 10 μg/ml each of aprotinin and leupeptin, 1 mM PMSF). Lysates were centrifuged as described above, equal volumes were incubated with the GST-Rho binding domain of Rhotekin (RBD) beads (20 μg protein/sample) for 45 min at 4°C, washed three times, and eluted with SDS sample buffer. Rho protein was detected by Western blotting using a polyclonal antibody against RhoA (Santa Cruz Biotechnology). Densitometry analysis was performed using Scion Image software (Scion Corporation).

Fluorescence microscopy

Cells were fixed for 20 min in 2% formaldehyde in PBS. For the cells on the stretch apparatus, the silicone membrane was adhered to slide glass

with 732 multipurpose sealant (Dow Corning) at 4°C for 16 h. Cells were then permeabilized for 5 min with 0.2% Triton X-100/PBS, and were stained for 60 min in either 1:250 or 1:500 dilution of rhodamine-phalloidin (Molecular Probes). Images were recorded using a BioRad 1024 confocal microscope with a 60× SPlanApo 60 PL oil objective.

Quantification of lamellipodia

Cells stained with rhodamine-phalloidin were analyzed by either Inovision ISEE imaging software (Inovision) or Image Pro Plus software program (Media Cybernetics). Both the total cell periphery and the portion of the periphery occupied with lamellipodia were outlined. The percentage of lamellipodia was defined as: (the length of perimeter occupied by lamellipodia/total perimeter) × 100.

Real-time video phase-contrast microscopy

VSM cells were spread on collagen I–coated silicone membranes in either the equibiaxial or uniaxial stretch device. They were placed in an open chamber with atmospheric and temperature control (Schwartz, 1993) before and after the stretch. Cells were filmed from 10 min before to 70 min after the stretch at a 1-min interval with a Nikon DiaPhot microscope equipped with a SenSys cooled CCD video camera linked to a Silicon Graphics workstation running the Inovision ISEE software program (Kiosses et al., 1999). To calculate areas, cells were outlined manually in phase contrast images and areas within the boundary determined by the software.

Cells and microscopy for FRET assays

VSM cells were plated in 6-cm cell culture dishes and were transfected with 2 μg of pEGFP-C1 wild- type Rac with 3.3 mM thymidine to synchronize the cell cycle to enhance transfection efficiency (Goldstein et al., 1989). After the transfection, 5 mM of sodium butyrate was added to enhance expression (Goldstein et al., 1989). After 24 h, cells were trypsinized and were adjusted to 4×10^5 cells/ml. To one ml was added 3.75 μg of Alexa-PBD and cells were sheared through a 27-gauge needle as described (Clarke and McNeil, 1992). Cells were plated on collagen I–coated silicone membrane assembled in the uniaxial stretch device. At 75 min after plating, cells were stretched by 8% for the indicated time, and fixed with 2% formaldehyde in PBS.

FRET analysis

Imaging was performed using a BioRad 1024 Confocal Microscope where the filters were optimized to best acquire the GFP-, FRET-, and Alexa 546–labeled images of cells (Del Pozo et al., 2002). These filters are: (1) GFP-Rac, excitation 488, emission 522; (2) Alexa 546, excitation 568, emission 598; and (3) FRET, excitation 488, emission 598. GFP and FRET images were acquired simultaneously, and Alexa 546 images were acquired separately, at the same plane and without any shift in the sample. GFP and FRET images of cells injected with GFP Rac only, and Alexa and FRET images of cells injected with Alexa PBD only were also obtained in order to determine bleed through and background levels to correct the initial FRET images (Chamberlain et al., 2000; Kraynov et al., 2000). These calculations were made using the ISEE software running on a UNIX workstation. Corrected FRET images on an 8-bit, 512 × 512 scale typically had a fluorescence intensity range of 0–92 in these experiments. This fluorescence intensity range was displayed using a color spectrum, where blue was closest to 0 and red was closest to 92. Positive FRET signals typically appeared between 46 and 92, in the green-yellow to red range. Below that was considered baseline.

Real-time video phase-contrast microscopy to quantify lamellipodia of living cells

To assay lamellipodia, VSM cells were plated on coverslips coated with collagen I. Dishes were prepared by cutting a hole in the bottom of the dish and attaching a coverslip to the outside of the dish with silicon grease. These were placed in an open chamber with temperature control. The medium was replaced by Hepes medium to keep a physiologic pH without CO_2. Cells were viewed with an Olympus IX70 microscope equipped with a coolSNAP-Pro camera (Media Cybernetics), linked to a Gateway computer running the Image Pro Plus software program. Cell morphology was assayed by time-lapse imaging (one image per minute) 20 min before treatment and 60–80 min after treatment. To quantify lamellipodia, the portion of the cell periphery with and without lamellipodia were outlined separately using the Image Pro Plus software program. The length of total lamellipodia and lamellipodia at the tail (defined as the region located behind the nucleus), and the length of the total perimeter of the cell were compiled for multiple cells. The percentage of lamellipodia was defined as: (the length of total or tail lamellipodia/total perimeter) × 100.

Measurements of traction and contractile force

Contractile forces were measured using flexible polyacrylamide substrates (5% acrylamide and 0.1% Bis-acrylamide) containing fluorescent beads as described (Wang et al., 2002). Cells were plated on collagen I–coated polyacrylamide and treated with ML-7 or Y-27632 for 1h. At the end of the experiment, cell-generated traction was eliminated by adding 1% SDS at final concentration. Calculations of traction forces were done as described (Butler et al., 2002).

We thank Dr. John Collard (Netherlands Cancer Institute) for providing pcDNAINeo-Tiam1, and Drs. Sanford J. Shattil and Mark H. Ginsberg for critical reading of manuscript. We thank Dr. Ning Wang (Harvard School of Public Health) for providing the software for traction force calculations. We thank Ms. Nazilla Alderson for preparing DNA constructs and GST–PBD and Alexa-PBD proteins, and Ms. Bette Cessna for excellent secretarial assistance.

This work was supported by USPHS grant P01HL57900 (to M.A. Schwartz), GM57464 (to K.M. Hahn), Uehara Memorial Foundation (to A. Katsumi), Association pour la recherché contre Le cancer (to J. Milanini), EMBO (to M.A. del Pozo), Leukemia and Lymphoma Society Special Fellowship #3347-02 (to M.A. del Pozo), and American Heart Association fellowship 0120069Y (to W.B. Kiosses).

Submitted: 23 January 2002
Revised: 16 May 2002
Accepted: 17 May 2002

References

Balaban, N.Q., U.S. Schwarz, D. Riveline, P. Goichberg, G. Tzur, I. Sabanay, D. Mahalu, S. Safran, A. Bershadsky, L. Addadi, and B. Geiger. 2001. Force and focal adhesion assembly: a close relationship studied using elastic micropatterned substrates. *Nat Cell Biol.* 3:466–472.

Bray, D. 1984. Axonal growth in response to experimentally applied mechanical tension. *Dev. Biol.* 102:379–389.

Bray, D., and J.G. White. 1988. Cortical flow in animal cells. *Science.* 239:883–888.

Butler, J.P., I.M. Tolic-Norrelykke, B. Fabry, and J.J. Fredberg 2002. *Am. J. Cell Physiol.* 282:C595–C605.

Chamberlain, C.E., V.S. Kraynov, and K.M. Hahn. 2000. Imaging spatiotemporal dynamics of Rac activation in vivo with FLAIR. *Methods Enzymol.* 325:389–400.

Clarke, M.S., and P.L. McNeil. 1992. Syringe loading introduces macromolecules into living mammalian cell cytosol. *J. Cell Sci.* 102:533–541.

Cox, E.A., S.K. Sastry, and A. Huttenlocher. 2001. Integrin-mediated adhesion regulates cell polarity and membrane protrusion through the Rho family of GTPases. *Mol. Biol. Cell.* 12:265–277.

Davies, P.F. 1995. Flow-mediated endothelial mechanotransduction. *Physiol. Rev.* 75:519–560.

Davis, G.E., and C.W. Camarillo. 1995. Regulation of endothelial cell morphogenesis by integrins, mechanical forces, and matrix guidance pathways. *Exp. Cell Res.* 216:113–123.

Del Pozo, M.A., W.B. Kiosses, N.B. Alderson, N. Meller, K.M. Hahn, and M.A. Schwartz. 2002. Integrins regulate GTP-Rac localized effector interactions through dissociation of Rho-GDI. *Nat. Cell Biol.* 4:232–239.

del Pozo, M.A., M. Vicente-Manzanares, R. Tejedor, J.M. Serrador, and F. Sanchez-Madrid. 1999. Rho GTPases control migration and polarization of adhesion molecules and cytoskeletal ERM components in T lymphocytes. *Eur. J. Immunol.* 29:3609–3620.

del Pozo, M.A., L.S. Price, N.B. Alderson, X.D. Ren, and M.A. Schwartz. 2000. Adhesion to the extracellular matrix regulates the coupling of the small GTPase Rac to its effector PAK. *EMBO J.* 19:2008–2014.

Galbraith, C.G., and M.P. Sheetz. 1997. A micromachined device provides a new bend on fibroblast traction forces. *Proc. Natl. Acad. Sci. USA.* 94:9114–9118.

Goldstein, S., C.M. Fordis, and B.H. Howard. 1989. Enhanced transfection efficiency and improved cell survival after electroporation of G2/M-synchronized cells and treatment with sodium butyrate. *Nucleic Acids Res.* 17:3959–3971.

Haston, W.S., J.M. Shields, and P.C. Wilkinson. 1983. The orientation of fibro-

blasts and neutrophils on elastic substrata. *Exp. Cell Res.* 146:117–126.

Ingber, D.E. 1997. Tensegrity: the architectural basis of cellular mechanotransduction. *Annu. Rev. Physiol.* 59:575–599.

Ingber, D.E., and J. Folkman. 1989. How does extracellular matrix control capillary morphogenesis? *Cell.* 58:803–805.

Kiosses, W.B., R.H. Daniels, C. Otey, G.M. Bokoch, and M.A. Schwartz. 1999. A role for p21-activated kinase in endothelial cell migration. *J. Cell Biol.* 147: 831–844.

Kolega, J. 1986. Effects of mechanical tension on protrusive activity and microfilament and intermediate filament organization in an epidermal epithelium moving in culture. *J. Cell Biol.* 102:1400–1411.

Kraynov, V.S., C. Chamberlain, G.M. Bokoch, M.A. Schwartz, S. Slabaugh, and K.M. Hahn. 2000. Localized Rac activation dynamics visualized in living cells. *Science.* 290:333–337.

Lane Smith, R., M.C. Trindade, T. Ikenoue, M. Mohtai, P. Das, D.R. Carter, S.B. Goodman, and D.J. Schurman. 2000. Effects of shear stress on articular chondrocyte metabolism. *Biorheology.* 37:95–107.

Lee, A.A., T. Delhaas, A.D. McCulloch, and F.J. Villarreal. 1999. Differential responses of adult cardiac fibroblasts to in vitro biaxial strain patterns. *J. Mol. Cell. Cardiol.* 31:1833–1843.

Lee, A.A., T. Delhaas, L.K. Waldman, D.A. MacKenna, F.J. Villarreal, and A.D. McCulloch. 1996. An equibiaxial strain system for cultured cells. *Am. J. Physiol.* 271:C1400–C1408.

Narumiya, S., T. Ishizaki, and M. Uehata. 2000. Use and properties of ROCK-specific inhibitor Y-27632. *Methods Enzymol.* 325:273–284.

Naruse, K., T. Yamada, and M. Sokabe. 1998. Involvement of SA channels in orienting response of cultured endothelial cells to cyclic stretch. *Am. J. Physiol.* 274:H1532–H1538.

Pelham, R.J., Jr., and Y. Wang. 1997. Cell locomotion and focal adhesions are regulated by substrate flexibility. *Proc. Natl. Acad. Sci. USA.* 94:13661–13665.

Pelham, R.J., Jr., and Y. Wang. 1999. High resolution detection of mechanical forces exerted by locomoting fibroblasts on the substrate. *Mol. Biol. Cell.* 10: 935–945.

Pitelka, D.R., and B.N. Taggart. 1983. Mechanical tension induces lateral movement of intramembrane components of the tight junction: studies on mouse mammary cells in culture. *J. Cell Biol.* 96:606–612.

Price, L.S., J. Leng, M.A. Schwartz, and G.M. Bokoch. 1998. Activation of Rac and Cdc42 by integrins mediates cell spreading. *Mol. Biol. Cell.* 9:1863–1871.

Ren, X.D., W.B. Kiosses, and M.A. Schwartz. 1999. Regulation of the small GTP-binding protein Rho by cell adhesion and the cytoskeleton. *EMBO J.* 18: 578–585.

Riveline, D., E. Zamir, N.Q. Balaban, U.S. Schwarz, T. Ishizaki, S. Narumiya, Z. Kam, B. Geiger, and A.D. Bershadsky. 2001. Focal contacts as mechanosensors: externally applied local mechanical force induces growth of focal contacts by an mDia1-dependent and ROCK-independent mechanism. *J Cell Biol.* 153:1175–1186.

Sadoshima, J., and S. Izumo. 1997. The cellular and molecular response of cardiac myocytes to mechanical stress. *Annu. Rev. Physiol.* 59:551–571.

Sadoshima, J., L. Jahn, T. Takahashi, T.J. Kulik, and S. Izumo. 1992. Molecular characterization of the stretch-induced adaptation of cultured cardiac cells. An in vitro model of load-induced cardiac hypertrophy. *J. Biol. Chem.* 267: 10551–10560.

Sai, X., K. Naruse, and M. Sokabe. 1999. Activation of pp60(src) is critical for stretch-induced orienting response in fibroblasts. *J. Cell Sci.* 112:1365–1373.

Schwartz, M.A. 1993. Spreading of human endothelial cells on fibronectin or vitronectin triggers elevation of intracellular free calcium. *J. Cell Biol.* 120: 1003–1010.

Schwartz, M.A., and S.J. Shattil. 2000. Signaling networks linking integrins and rho family GTPases. *Trends Biochem. Sci.* 25:388–391.

Shirinsky, V.P., A.S. Antonov, K.G. Birukov, A.V. Sobolevsky, Y.A. Romanov, N.V. Kabaeva, G.N. Antonova, and V.N. Smirnov. 1989. Mechano-chemical control of human endothelium orientation and size. *J. Cell Biol.* 109: 331–339.

Terracio, L., B. Miller, and T.K. Borg. 1988. Effects of cyclic mechanical stimulation of the cellular components of the heart: in vitro. *In Vitro Cell. Dev. Biol.* 24:53–58.

van Leeuwen, F.N., R.A. van der Kammen, G.G. Habets, and J.G. Collard. 1995. Oncogenic activity of Tiam1 and Rac1 in NIH3T3 cells. *Oncogene.* 11: 2215–2221.

Wang, H.B., M. Dembo, S.K. Hanks, and Y. Wang. 2001a. Focal adhesion kinase is involved in mechanosensing during fibroblast migration. *Proc. Natl. Acad. Sci. USA.* 98:11295–11300.

Wang, J.G., M. Miyazu, E. Matsushita, M. Sokabe, and K. Naruse. 2001b. Uniaxial cyclic stretch induces focal adhesion kinase (fak) tyrosine phosphorylation followed by mitogen-activated protein kinase (mapk) activation. *Biochem. Biophys. Res. Commun.* 288:356–361.

Wang, N., I.M. Tolic-Norrelykke, J. Chen, S.M. Mijailovich, J.P. Butler, J.J. Fredberg, and D. Stamenovic. 2002. Cell prestress. I. Stiffness and prestress are closely associated in adherent contractile cells. *Am. J. Physiol. Cell Physiol.* 282:C606–C616.

Wilson, E., K. Sudhir, and H.E. Ives. 1995. Mechanical strain of rat vascular smooth muscle cells is sensed by specific extracellular matrix/integrin interactions. *J. Clin. Invest.* 96:2364–2372.

Yano, Y., Y. Saito, S. Narumiya, and B.E. Sumpio. 1996. Involvement of rho p21 in cyclic strain-induced tyrosine phosphorylation of focal adhesion kinase (pp125FAK), morphological changes and migration of endothelial cells. *Biochem. Biophys. Res. Commun.* 224:508–515.

Zhong, C., M.S. Kinch, and K. Burridge. 1997. Rho-stimulated contractility contributes to the fibroblastic phenotype of Ras-transformed epithelial cells. *Mol. Biol. Cell.* 8:2329–2344.